ELSEVIER

Journal of Alloys and Compounds 321 (2001) 46–53

Journal of ALLOYS AND COMPOUNDS

www.elsevier.com/locate/jallcom

Hydrogen desorption behavior from magnesium hydrides synthesized by reactive mechanical alloying

F.C. Gennari[a,*], F.J. Castro[b], G. Urretavizcaya[a]

[a]*Consejo Nacional de Investigaciones Científicas y Técnicas, CONICET, 8400 S.C. de Bariloche, Río Negro, Argentina*
[b]*Departamento Tecnología de Materiales y Dispositivos, Centro Atómico Bariloche, CNEA, 8400 S.C. de Bariloche, Río Negro, Argentina*

Received 9 October 2000; accepted 26 October 2000

Abstract

The β- and γ-phases of MgH_2 were synthesized by reactive mechanical alloying (RMA) at room temperature under hydrogen atmosphere. The structural and desorption properties of the products obtained were examined by X-ray diffraction (XRD), differential scanning calorimetry (DSC), thermogravimetric analysis (TG) and scanning electron microscopy (SEM). Reactive mechanical alloying of Mg leads to the formation of about 50 wt.% of MgH_2 (β- and γ-phases) after 50 h of milling. Different thermal behaviors are observed depending on the milling time. Hydrogen thermal desorption shows a sharp endothermic peak for MgH_2 milled up to 30 h associated with β-MgH_2. For longer milling times, two endothermic peaks (or a double peak) are observed and are associated with hydrogen desorption from the γ-MgH_2–β-MgH_2 mixture and the β-MgH_2 phase. The presence of γ-MgH_2 destabilizes the β-MgH_2 phase, reducing its desorption temperature. The results of this study are consistent with hydrogen desorption from γ-MgH_2 prior to the γ→β-MgH_2 transformation.

Keywords: Magnesium hydride; Mechanical alloying; Hydrogen desorption; Differential scanning calorimetry; Thermal analysis

1. Introduction

Magnesium hydride (MgH_2) is an attractive energy storage material due to its high hydrogen storage capacity (7.6 wt.%) and large formation enthalpy ($\Delta H = -75$ kJ mol^{-1}). However, its slow hydriding/dehydriding kinetics and high dissociation temperature limit its use for hydrogen-related applications. One approach to improve the reaction kinetics of this material is reactive mechanical milling. The formation of a hydrogen-absorbing material by mechanical milling under hydrogen atmosphere simultaneously produces hydrogen uptake, mechanical deformation, defect formation and surface modification [1–4]. These structural modifications can lead to the formation of metastable phases, refinement of the microstructure into the nanometer range, extension of solubility limits, development of amorphous phases, etc. [5–7]. These effects produce important changes in the hydrogen-absorption and -desorption properties.

In order to understand the structural changes that occur during RMA (reactive mechanical alloying), the known phases of the system Mg–H should be analyzed first. The temperature–composition diagram of the Mg–H system consists of a hcp α-phase (interstitial solid solution) and a β-phase with tetragonal structure and a stoichiometric nominal composition of MgH_2 [8]. When the tetragonal β-MgH_2 phase is subjected to high compressive stress, it partially transforms into the metastable orthorhombic γ-phase [9]. The transition β→γ was also observed at a pressure of 2.5 GPa. Both phases coexist up to a pressure of 8 GPa [8,9]. The metastable γ-phase reverts exothermically to the tetragonal β-phase by heating at 350°C, as measured by DTA between 300 and 350°C [9]. Another metastable MgH_2 phase, the hexagonal (pseudocubic) δ-phase, has been observed after treatment of the β-phase at 2.8 to 8 GPa and 650 to 800°C [8]. The thermal study of Bastides et al. [9] on a β–δ-MgH_2 mixture showed an endothermic effect between 350 and 400°C. This effect was attributed either to δ→γ or to δ→β phase transitions.

In the present work, we studied the thermal desorption

*Corresponding author. Centro Atómico Bariloche, Departamento Tecnologia de Materiales y Dispositivos, 8400 S.C. de Bariloche, Río Negro, Argentina. Tel.: +54-944-610-025; fax: +54-944-610-06.
E-mail address: gennari@cab.cnea.gov.ar (F.C. Gennari).

0925-8388/01/$ – see front matter
PII: S0925-8388(00)01460-2

behavior of MgH_2 hydrides produced by RMA, and related the structural and microstructural changes induced by mechanical milling to the thermal stability of the hydrides.

2. Experimental

Elemental magnesium granules (purity >99.9%) were mechanically milled under hydrogen atmosphere using a Uni-Ball-Mill II apparatus (Australian Scientific Instruments). The Mg granules together with ferromagnetic steel balls were placed in a stainless steel container enclosed in an argon glove box. The container was then evacuated to 10^{-5} MPa prior to filling with 0.5 MPa of high-purity hydrogen (99.995%, Air Liquide). The samples were milled for different times up to 100 h and the container was systematically refilled with hydrogen every 5 h in order to keep the hydrogen pressure constant. The ball-to-powder weight ratio was 44:1.

At regular intervals, the container was opened in an argon glove box and a small amount of powder was taken for analysis by X-ray powder diffraction (XRD), scanning electron microscopy (SEM) and differential scanning calorimetry (DSC). The X-ray powder diffraction was performed using a Philips PW 1710/01 instrument with Cu Kα radiation (graphite monochromator). Scanning electron microscopy (SEM 515, Philips Electronic Instruments) was used to characterize the microstructure. The thermal behavior of the samples was studied by DSC (DSC 2910, TA Instruments) at a heating rate of 6°C min^{-1} and an argon flow rate of 18 ml min^{-1}. The proportion of MgH_2 was calculated using the peak area of the DSC curves and the reported MgH_2 heat of formation (75 kJ mol^{-1}, [10]). Also, thermogravimetric (TG) analyses were carried out under argon atmosphere at a heating rate of 6°C min^{-1} and an argon flow rate of 50 ml min^{-1}.

3. Results and discussion

3.1. Formation of β-MgH_2 and γ-MgH_2

The evolution of the X-ray diffraction patterns as a function of milling time for Mg milled in hydrogen atmosphere is shown in Fig. 1. Tetragonal β-MgH_2 (JCPDS 12-0697) is formed in the initial period of milling (15 h). The presence of this phase is even more evident after 35 h by the increase of the relative intensities of the (110), $2\theta = 27.97°$ and (101), $2\theta = 35.77°$ diffraction peaks. The half height width of these peaks increases with milling time, indicating that the β-MgH_2 crystallite size decreases. Crystalline residual magnesium (JCPDS 35-0821) is still detected after up to 50 h of milling. The appearance of MgO (JCPDS 45-0946) is observed after 35 h of milling, probably due to the presence of oxygen in the

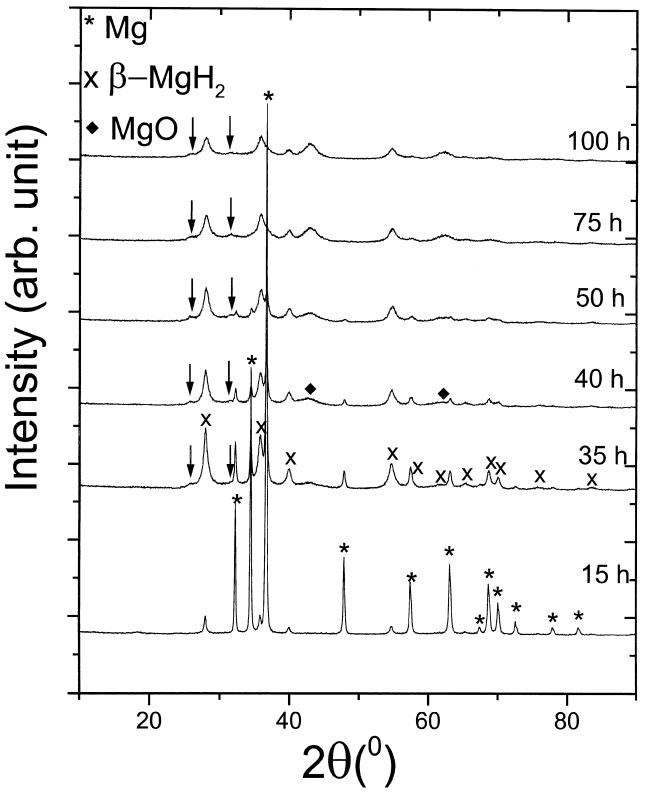

Fig. 1. X-ray diffraction patterns of Mg after RMA as a function of milling time. The γ-MgH_2 phase peaks are indicated by arrows.

starting powder and the high reactivity of magnesium. No further structural changes are observed between 75 and 100 h of milling. Table 1 summarizes the phases detected by XRD and the β-MgH_2 crystallite size (calculated using the Scherrer equation [11]) as a function of milling time.

An interesting result is that orthorhombic γ-MgH_2 (JCPDS 35-1184) is detected simultaneously with β-MgH_2 from 35 h of milling. Fig. 2 shows in detail the peaks corresponding to γ-MgH_2 formed after RMA for different milling times (the XRD patterns were recorded with more statistics and precision). The broadening of the X-ray peaks associated with the reduction of the crystal size is also observed for the γ-MgH_2 phase for milling times longer than 50 h. The γ-MgH_2 structure has been synthesized under high compression stress [9] from the β-phase. Recently, it has been observed under mechanical milling of β-MgH_2 in argon atmosphere at room temperature [12]. In our case, the structural defects and the mechanical deformations that occur during milling under hydrogen atmosphere produce the metastable orthorhombic γ-phase. These modifications also have an effect on the hydrogen desorption process, as will be analyzed in the following section.

Confirmation of the morphological changes produced by RMA after 15, 35 and 100 h can be seen from Figs. 3 and 4. Wide area micrographs (Fig. 3) show that particle size decreases for longer milling times, from 50–150 μm for

Table 1
Phases detected by XRD, crystallite size and characteristic thermal desorption temperatures of MgH_2 as a function of milling time

Milling time (h)	Phases detected by XRD before DSC measurement	Crystallite size of β-MgH_2 (Å)	DSC			
			MgH_2 (wt.%)	T_{onset} (°C)	T_{peak} (°C)	
					Peak 1	Peak 2
15	β-MgH_2, Mg	290	5.8	422	–	444
20	β-MgH_2, Mg	–	10.4	432	–	435
25	β-MgH_2, Mg	–	21.0	428	–	433
35	β-MgH_2, γ-MgH_2, Mg, MgO	143	39.5	385	404	426
40	β-MgH_2, γ-MgH_2, Mg, MgO	–	46	382	404	430
50	β-MgH_2, γ-MgH_2, Mg, MgO	106	49.2	368	400	430
60	β-MgH_2, γ-MgH_2, Mg, MgO	–	54.7	393	404	426
75	β-MgH_2, γ-MgH_2, MgO	99	47.4	389	394	420
100	β-MgH_2, γ-MgH_2, MgO	91	48.4	381	388	407

15 h of milling to 5–50 μm for 35 h of milling. In the first milling stages (up to 15 h), mechanical alloying is mainly performed on ductile Mg. In this case, the milling produces a slight decrease of particle size (Fig. 3A). However, at 35 h of milling we observe a significant decrease in particle size (Fig. 3B). This is a consequence of the embrittlement associated with hydride formation [1,13,14], as observed from the XRD patterns (Fig. 1) after 35 h of milling. The reduction in particle size results in an increase of the specific area for hydrogen absorption. The increment in the specific area has an additional contribution, as shown in Fig. 4. The micrograph corresponding to 15 h of milling (Fig. 4A) shows an aggregated particle with laminar structure due to the cold welding phenomena occurring in the initial stage of mechanical alloying. For longer milling times (35 and 100 h), almost spherical porous particles with ultrafine grains characterize the surface. The average crystallite sizes are 290, 143 and 91 Å for 15, 35 and 100 h of milling, respectively (see Table 1).

3.2. Desorption behavior of MgH_2 synthesized by RMA

DSC measurements of the MgH_2 samples corresponding to different milling times are shown in Fig. 5. The amount of MgH_2, the onset temperature (T_{onset}) of the endothermic peaks and the temperature of the peaks (T_{peak}) as a function of milling time obtained from these curves are summarized in Table 1. XRD analyses performed on the

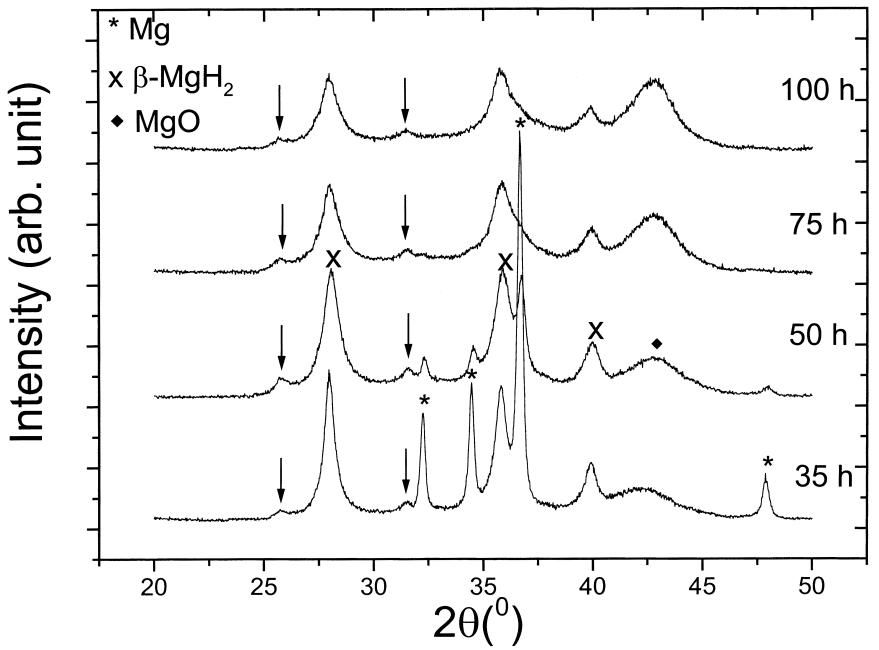

Fig. 2. Selected X-ray diffraction patterns of Mg after RMA obtained with more statistics and precision for various milling times. The γ-MgH_2 phase peaks are indicated by arrows.

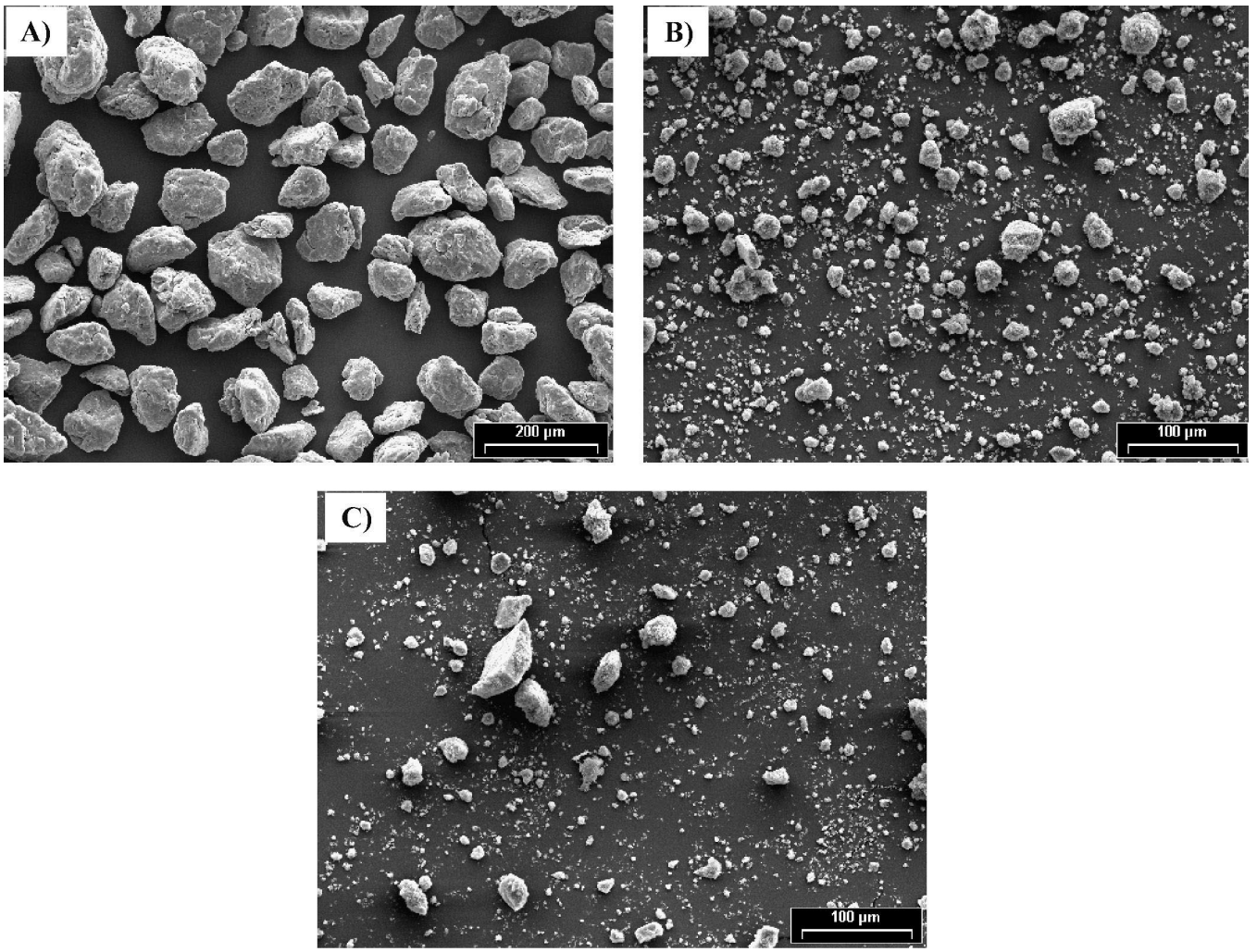

Fig. 3. Wide area SEM micrographs of Mg after RMA for different milling times. (A) 15 h, (B) 35 h, and (C) 100 h.

samples after complete DSC measurements show Mg and MgO as the only residual phases. This confirms that MgH_2 completely decomposes during heating.

We identify in Fig. 5 three different types of behavior during MgH_2 decomposition as a function of milling time. The first desorption behavior (Fig. 5A) corresponds to DSC curves obtained from samples milled for times shorter than 35 h. There we identify only a sharp endothermic peak at 444°C (15 h) and 433°C (25 h) (see Table 1). The second type of behavior (Fig. 5B) corresponds to DSC curves obtained from samples milled from 35 to 50 h. In this case we see a shallow low-temperature peak (ca. 400°C) and a sharp high-temperature peak (ca. 430°C) (see Table 1). The third type of behavior (Fig. 5C) consists of a double endothermic peak observed when the milling time goes beyond 50 h. For the sample milled for 100 h the peak temperatures are 388 and 407°C (Table 1). As a general characteristic of each type of behavior, T_{onset} and T_{peak} decrease with milling time.

The sharp endothermic peak observed for samples milled for less than 35 h (Fig. 5A) is assigned to the decomposition of β-MgH_2, in accordance with the XRD results (Table 1). This observation agrees with previous thermal studies [3,13]. Huot et al. [3] found that MgH_2 formed by RMA presents an endothermic peak with an onset temperature around 441°C. Similarly, Zaluska et al. [13] observed an endothermic peak near 400°C. In both investigations, the peaks correspond to MgH_2 decomposition and the only hydride present in the sample was β-MgH_2. Additionally, we observe a peak shift towards lower temperatures due to particle size reduction (Figs. 3 and 4) and the microstructural modifications induced by RMA.

The DSC curves for the samples milled between 30 and 50 h (Fig. 5B, second type of behavior) show two endothermic peaks: a low-temperature peak (peak 1, Table 1) and a high-temperature peak (peak 2, Table 1). This behavior shows that two processes with different kinetics are occurring. From the similarity between the sharp endothermic peak of Fig. 5A and the high-temperature peak of Fig. 5B, we attribute this last peak to β-MgH_2 decomposition. On the other hand, a correlation between the presence of γ-MgH_2 (Table 1) and the appearance of the low-temperature peak is observed.

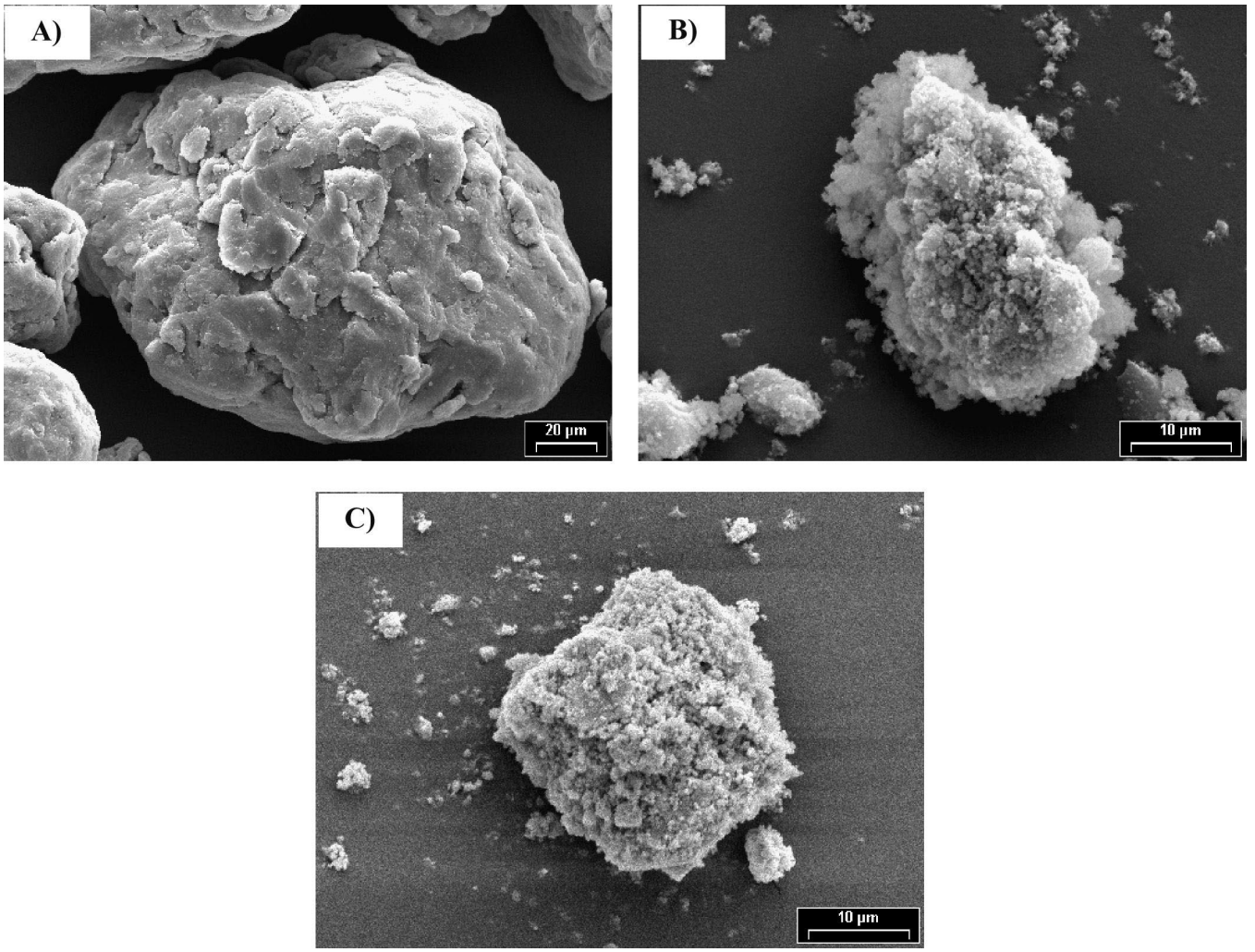

Fig. 4. Local area SEM micrographs of Mg after RMA for different milling times. (A) 15 h, (B) 35 h, and (C) 100 h.

In order to clarify the nature of the endothermic phenomena, two different studies were performed: TG and XRD analysis on samples taken after partial DSC measurement. Fig. 6 shows the TG curve of MgH_2 formed by RMA after 50 h of milling. The total relative weight loss is about 4.9% and is associated with hydrogen desorption. This result is in agreement with the amount of hydrogen determined from DSC measurement: 4.7 wt.% H (or 49.2 wt.% MgH_2, Table 1). From the DSC (Fig. 5B) and TG (Fig. 6) curves, the onset temperatures of desorption are 368 and 350°C, respectively. The temperature difference can be attributed to the fact that sample preparation and disposal were different for each technique. Considering these characteristics, the TG curve shows that both endothermic peaks have an associated mass loss and can only be related to hydrogen desorption processes (MgH_2 decomposition).

As mentioned above, the structural changes occurring during DSC measurement in the sample milled for 50 h were monitored by XRD. Three different DSC runs were stopped at 370, 420 and 500°C. The XRD patterns are shown in Fig. 7. The sample heated to 370°C shows the presence of the γ-MgH_2 and β-MgH_2 phases. The exothermic effect reported by Bastides et al. [9] due to the γ→β transformation was not observed. The sample heated to 420°C presents free Mg, MgO and β-MgH_2. The diffraction peaks corresponding to γ-MgH_2 were not detected. Partial hydrogen desorption from β-MgH_2 has already started at 420°C, as can be inferred from the decrease in the intensity of the β-MgH_2 peaks at 420°C with respect to 370°C (referred to MgO). At 500°C, β-MgH_2 decomposition is complete and only Mg and MgO were detected as residual phases. The XRD and TG studies demonstrate that the low-temperature DSC peak is due to the total decomposition of γ-MgH_2 and the partial decomposition of β-MgH_2, whereas the high-temperature DSC peak corresponds to β-MgH_2 decomposition, as inferred previously. The second type of desorption be-

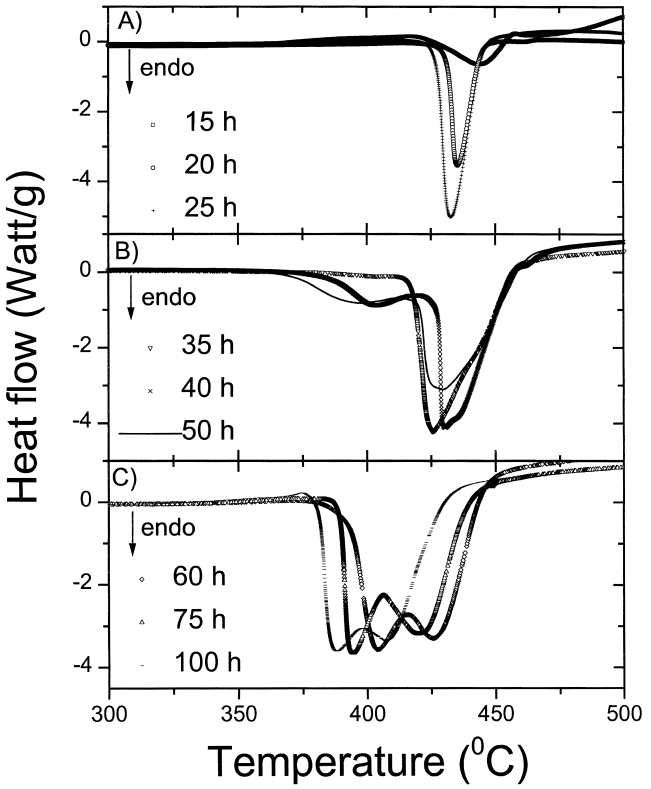

Fig. 5. DSC curves of Mg after RMA as a function of milling time. (A) From 15 to 30 h, (B) from 35 to 50 h, and (C) from 60 to 100 h.

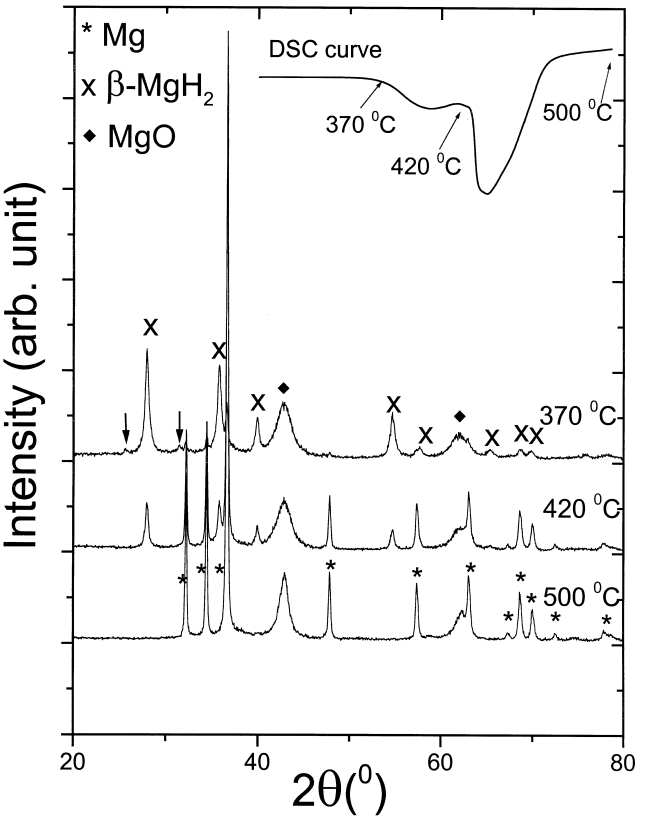

Fig. 7. XRD patterns of Mg after 50 h of RMA obtained after DSC runs stopped at 370, 420 and 500°C. The γ-MgH_2 phase peaks are indicated by arrows.

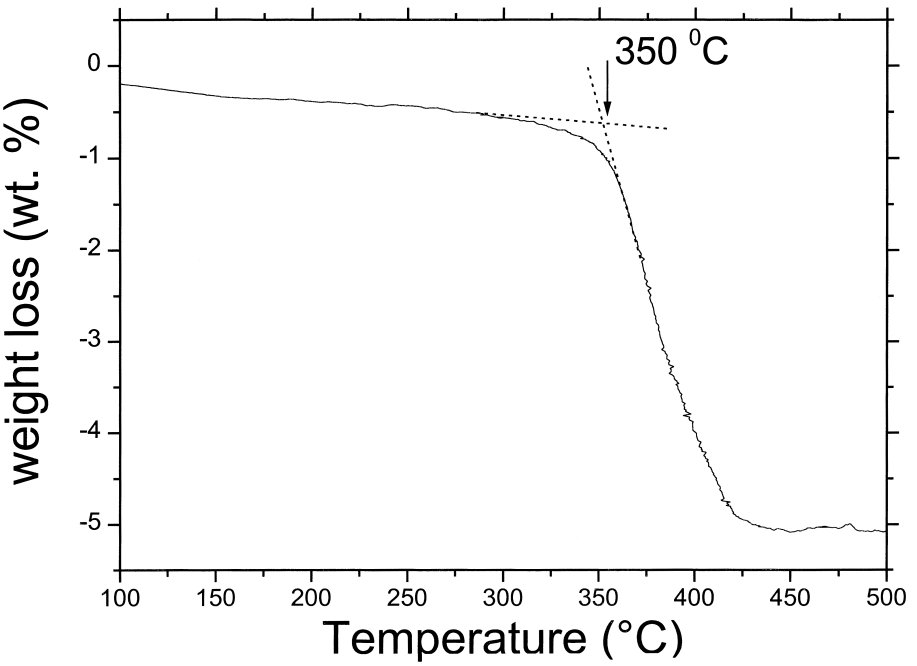

Fig. 6. TG curve of Mg after RMA milling for 50 h.

havior (Fig. 5B) then suggests that the metastable γ-MgH_2 phase destabilizes stable β-MgH_2, resulting in its partial decomposition at the temperature at which γ-MgH_2 decomposes.

Similarly, the low-temperature peak observed in the DSC runs of samples milled between 60 and 100 h (third type of behavior, Fig. 5C) is due to γ-MgH_2 and β-MgH_2 decomposition. To confirm this, we stopped three DSC runs at 380, 385 and 390°C of the sample milled for 100 h, and analyzed the corresponding XRD patterns (Fig. 8). The γ-MgH_2 phase was only detected in the samples heated to 380 and 385°C, showing that γ-MgH_2 totally decomposes when heated to 390°C. For the samples heated to 385 and 390°C, the relative intensities of the peaks associated with the β-MgH_2 phase decrease, while those corresponding to Mg increase (taking the most intense MgO peak as reference). Then, for the third type of thermal behavior, the low-temperature DSC peak represents hydrogen desorption from both γ-MgH_2 and β-MgH_2, and the high-temperature effect is attributed to the desorption from β-MgH_2. The double peak shown in Fig. 5C is similar to that found by Huot et al. [12] during the decomposition of a β-MgH_2 and γ-MgH_2 mixture produced by milling under argon atmosphere; however, these authors did not explain this splitting. The second type of behavior was not observed in this previous study [12], probably due to the use of a high energetic shaker mill. In contrast, our low-energy apparatus allows us to observe intermediate stages during RMA.

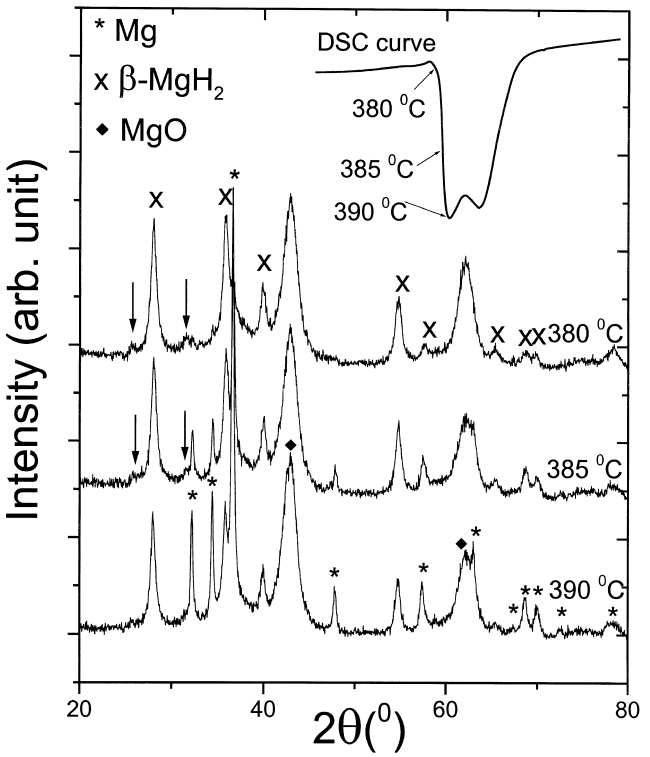

Fig. 8. XRD patterns of Mg after 100 h of RMA obtained after DSC runs stopped at 380, 385 and 390°C. The γ-MgH_2 phase peaks are indicated by arrows.

As shown in Table 1 and Fig. 2, the γ-phase starts to be detected from 35 h of milling. The wt.% of the MgH_2 phase is almost constant from 50 h of milling (Table 1). Then, between 35 and 50 h of RMA the formation of β-MgH_2 and γ-MgH_2 occurs simultaneously, and both processes are competitive. It has been reported previously [12] that the γ-phase is formed by β→γ transformation during milling under argon atmosphere. From our results it is not possible to establish if the γ-phase was formed by β→γ transformation and/or by direct synthesis from Mg.

We suggest that the presence of γ-MgH_2 produces a synergetic effect during hydrogen desorption that stimulates β-MgH_2 decomposition at lower temperatures. This effect is responsible for the appearance of the first peak in Fig. 5B,C. Synergetic behavior has been proposed previously by Zaluska et al. [13] when studying a mixture of β-MgH_2 and Mg_2NiH_4. In our system, the synergy of desorption could be due to the interaction between close neighbors of γ-MgH_2 and β-MgH_2. The metastable γ-MgH_2 phase decomposes before the stable β-MgH_2, producing a volume contraction. This process generates stresses that act on the attached β-MgH_2 clusters and facilitate β-MgH_2 decomposition [13].

No appreciable changes in the relative amounts of phases are detected when milling for more than 50 h. Mechanical milling only introduces significant internal, structural changes such as defects, micro-stresses and local imperfections. The broadening of the XRD peaks of the β-MgH_2 and γ-MgH_2 phases (Figs. 1 and 2) confirms the reduction of their grain size and the induction of microstresses during milling. Also, for milling times longer than 50 h the γ-MgH_2 and β-MgH_2 clusters formed during RMA are refined and intermixed inside newly formed particles. These microstructural changes produce an increase in the area of the first DSC peak that is observed when comparing the DSC curves of the second and third types of behavior (Fig. 5B,C, respectively). This increment represents a significant enhancement of the desorption kinetics of MgH_2. Possibly, there is an ''ideal'' composition of the γ-MgH_2 and β-MgH_2 mixture for which the amount of γ-MgH_2 affects all the β-MgH_2 phase present in the mixture. Our experimental results (Fig. 5B,C) suggest that this ideal composition has not been reached, because a certain amount of the β-MgH_2 phase still desorbs hydrogen at its usual temperature (second peak).

4. Conclusions

The stable β-MgH_2 and metastable γ-MgH_2 phases were synthesized by RMA in hydrogen atmosphere from Mg granules. The RMA process produces embrittlement of the material, particle and crystallite size reduction, a

specific surface increase and the formation of metastable γ-MgH_2.

The material shows three different types of desorption behavior associated with the structural changes produced during milling. For shorter milling times, when β-MgH_2 is the only hydride present, a sharp endothermic peak is observed. This peak is associated with hydrogen desorption from the β-MgH_2 phase. For longer milling times, when the presence of γ-MgH_2 and β-MgH_2 was detected simultaneously, two peaks or a double peak are observed. The low-temperature endothermic peak corresponds to the complete dehydriding of γ-MgH_2 and the partial dehydriding of β-MgH_2, whereas the high-temperature peak corresponds to hydrogen desorption from β-MgH_2. The γ-MgH_2 phase decomposes before the γ→β transformation. The detection of γ-MgH_2 at temperatures as high as 385°C indicates an extension of its metastability range with respect to that reported in the literature.

We propose that the γ-MgH_2 and β-MgH_2 mixture shows a synergetic effect during hydrogen desorption, which produces a decrease in the β-MgH_2 desorption temperature. This improvement of the hydrogen desorption properties becomes more significant as the milling time increases from 35 to 100 h, as a consequence of better phase intermixing of γ- and β-hydrides.

Acknowledgements

We wish to thank C. Cotaro and E. Scerbo for the SEM micrographs and X-ray diffraction patterns, respectively. The authors also thank J. Andrade Gamboa for critical reading of the manuscript.

References

[1] Y. Chen, J.S. Williams, J. Alloys Comp. 217 (1995) 181.
[2] P. Tessier, H. Enoki, M. Bououdina, E. Akida, J. Alloys Comp. 268 (1998) 285.
[3] J. Huot, E. Akida, T. Takada, J. Alloys Comp. 231 (1995) 815.
[4] A. Zaluska, L. Zaluski, J.O. Ström-Olsen, J. Alloys Comp. 288 (1999) 217.
[5] T. Massalski, H. Okamoto, P. Subramanian, L. Kacprzak (Eds.), Binary Alloy Phase Diagrams, 2nd Edition, American Society for Metals, Metals Park, OH, 1990, p. 2033.
[6] J.P. Bastide, B. Bonnetot, J.M. Létoffé, P. Claudy, Mater. Res. Bull. 15 (1980) 1779.
[7] C.C. Koch, in: R.W. Cahn (Ed.), Materials Science and Technology — A Comprehensive Treatment, Processing of Metals and Alloys, Vol. 15, VCH, Weinheim, 1991.
[8] F.H. Froes, C. Suryanarayana, K. Russell, C.G. Li, Mater. Sci. Eng. A 192–195 (1995) 612.
[9] L. Lü, M.O. Lai, Mechanical Alloying, Kluwer Academic, Boston, 1998.
[10] O. Kubaschewski, C.B. Alcock, Metallurgical Thermochemistry, 5th Edition, International Series on Materials Science and Technology, Vol. 24, Pergamon Press, Oxford, 1979.
[11] H.P. Klug, L. Alexander, X-ray Diffraction Procedures For Polycrystalline and Amorphous Materials, Wiley, New York, 1974.
[12] J. Huot, G. Liang, S. Boily, A. Van Neste, R. Schulz, J. Alloys Comp. 293 (1999) 495.
[13] A. Zaluska, L. Zaluski, J.O. Ström-Olsen, J. Alloys Comp. 289 (1999) 197.
[14] J.-L. Bobet, C. Even, Y. Nakamura, E. Akiba, B. Darriet, J. Alloys Comp. 298 (2000) 279.